Metabolic Effects of Mislocalized Mitochondrial and Peroxisomal Citrate Synthases in Yeast *Saccharomyces cerevisiae*[†]

Christian Vélot,*[,‡,§] Sandrine Lebreton,[‡,§,||] Igor Morgunov,[‡,§] Ken C. Usher,[⊥] and Paul A. Srere[‡,§,○]

The Research Service of the Department of Veterans Affairs Medical Center, 4500 South Lancaster Road, Dallas, Texas 75216, Department of Biochemistry, and the Howard Hughes Medical Institute, University of Texas Southwestern Medical Center, 5323 Harry Hines Boulevard, Dallas, Texas 75235

Received July 22, 1999; Revised Manuscript Received September 16, 1999

ABSTRACT: Genes *CIT1* and *CIT2* from *Saccharomyces cerevisiae* encode mitochondrial and peroxisomal citrate synthases involved in the Krebs tricarboxylic acid (TCA) cycle and glyoxylate pathway, respectively. A Δ*cit1* mutant does not grow on acetate, despite the presence of Cit2p that could, in principle, bypass the resulting block in the TCA cycle. To elucidate this absence of cross-complementation, we have examined the ability of Cit1p to function in the cytosol, and that of Cit2p to function in mitochondria. A cytosolically localized form of Cit1p was also incompetent for restoration of growth of a Δ*cit1* strain on acetate, suggesting that mitochondrial localization of Cit1p is essential for its function in the TCA cycle. Cit2p was able, when mislocalized in mitochondria, to restore a wild-type phenotype in a strain lacking Cit1p. We have purified these two isoenzymes as well as mitochondrial malate dehydrogenase, Mdh1p, and have shown that Cit2p was also able to mimic Cit1p in its *in vitro* interaction with Mdh1p. Models of Cit1p and Cit2p structures generated on the basis of that of pig citrate synthase indicate very high structural and electrostatic surface potential similarities between the two yeast isozymes. Altogether, these data indicate that metabolic functions may require structural as well as catalytic roles for the enzymes.

Citrate synthase (EC 4.1.3.7) catalyzes the condensation of acetyl coenzyme A and oxaloacetate to form citrate, the first step of the Krebs tricarboxylic acid (TCA)[1] cycle, the central metabolic pathway of aerobic organisms. Because of the 2-fold role of this cycle (oxidative by generating reducing equivalents that drive mitochondrial respiration and hence the synthesis of ATP, and biosynthetic by providing the carbon skeletons used in many anabolic pathways), citrate synthase (CS) is a key enzyme in cellular metabolism and is present in virtually all cells capable of oxidative metabolism. In mammalian cells, this reaction seems to be exclusively located in mitochondria. In yeast and plant cells, a second isozyme localized in peroxisomes is involved in the glyoxylate cycle, an anaplerotic pathway of the TCA cycle. The glyoxylate pathway enables synthesis of C_4 dicarboxylic acids from acetyl-CoA units, bypassing the two decarboxylation steps in the TCA cycle. Since the C_4 metabolites so produced can be used for energy production, gluconeogenesis and other biosynthetic pathways, the glyoxylate cycle allows cells to utilize C_2 compounds (such as acetate and ethanol) and fatty acids as sole carbon sources.

In yeast *Saccharomyces cerevisiae*, mitochondrial and extramitochondrial CS activities are encoded by distinct nuclear genes, *CIT1* (*1*) and *CIT2* (*2*, *3*), respectively. Later, it was clearly proven that Cit2p is localized in peroxisomes (*4*, *5*), and that its targeting to this organelle is mediated by its C-terminal tripeptide SKL (*6*). On the other hand, Cit1p, which shares 81% identity with Cit2p, ends in SKN and begins with a N-terminal mitochondrial signal sequence. Recently, Jia et al. (*7*) showed that a third gene, *CIT3*, encodes a second mitochondrial isoform of CS in *S. cerevisiae*, but the function and expression conditions of cit3p have not been elucidated.

A null *cit2* mutant is perfectly healthy and does not display any particular phenotype, whereas a *cit1* mutant does not grow on acetate as a sole carbon source. From a basic metabolic point of view (and even by ignoring the possible presence of Cit3p), this phenotype is unexpected since inner mitochondrial membrane is provided with a citrate transporter (*8*) that could allow Cit2p to act as a shunt for the missing Cit1p. This result is still more surprising since it is known that in a *cit1* strain, *CIT2* transcription and extramitochondrial CS activity are increased (*9*, *10*). Inability of yeast cells to grow on acetate occurs by disrupting almost any TCA cycle enzyme genes, including *MDH1*, which encodes malate dehydrogenase (MDH) (*11*) despite the fact that this enzyme

[†] This work was supported by Veterans Administration Research Service and NSF grant (MCB-9724922).

* To whom correspondence should be addressed: Dr. Christian Vélot, Dallas VA Medical Center, 4500 S. Lancaster Rd., Dallas, Texas 75216. Telephone: 214-857-0249. Fax: 214-372-9534. E-mail: poffenb1@airmail.net.

[‡] Dallas VA Medical Center.

[§] University of Texas Southwestern Medical Center.

[||] Current address: Institut Jacques Monod, Université Paris VI, tour 43, 2 place Jussieu, Paris 75005, France.

[⊥] Howard Hughes Medical Institute.

[○] Deceased.

[1] Abbreviations: BCA, bicinchoninic acid; BCIP, 5-bromo-4-chloro-3-indolyl phosphate; CS, citrate synthase; DTNB, dithionitrobenzoate; IDH, isocitrate dehydrogenase; IPTG, isopropyl β-D-thiogalactoside; LS, leader sequence; MDH, malate dehydrogenase; NBT, nitroblue tetrazolium; PAGE, polyacrylamide gel electrophoresis; PEG, poly(ethylene-glycol); PMSF, phenylmethylsulfonyl fluoride; SDS, sodium dodecyl sulfate; TCA, tricarboxylic acid; WT, wild-type.

10.1021/bi991695n CCC: $18.00
Published on Web 11/11/1999

also has isoforms (in the cytosol and peroxisomes) that could, in principle, bypass the resulting block in the cycle. Moreover, Kispal et al. (*12*) showed that the introduction in null *cit1* mutant cells of a catalytically inactive but structurally unchanged Cit1p protein results in restoration of TCA cycle function and growth on acetate. These studies are interpreted as indicating the presence of a complex of TCA cycle enzymes in which the structure of the outer surface of each enzyme is as important as the enzyme activity itself.

This idea of a TCA multienzyme complex allowing enzymatic reactions to occur via channeling of metabolites between enzyme active sites is supported by a large body of data (*13*, *14*). In the past few years, more evidence was presented concerning the interaction between sequential Krebs TCA cycle enzymes, and especially about channeling between CS and MDH. A genetically prepared bienzymatic fusion protein between yeast mitochondrial CS and MDH was shown to channel the intermediate oxaloacetate when compared to a solution of the free corresponding enzymes (*15*). This ability to channel oxaloacetate also was shown with pig CS and mitochondrial MDH maintained in a close proximity, either in a poly(ethylene glycol) (PEG) coprecipitate (*16*) or within a genetically prepared fusion enzyme (*17*). Moreover, in both strategies this channeling depends on ionic strength, which indicates an electrostatically based channeling mechanism. These results are consistent with the previous molecular modeling studies performed on the pig fusion enzyme by Brownian dynamics simulations, which provided evidence for the existence of an unbroken electrostatically favorable positive surface to guide oxaloacetate between the CS and MDH active sites (*18*). Recently, using a 5-fluorotryptophan labeled Cit1p in ^{19}F NMR, Haggie and Brindle (*19*) showed that this enzyme is motionally restricted in yeast mitochondria, consistent with its participation in a multienzyme complex.

To study further this TCA multienzyme complex hypothesis and to assess the ability of isoenzymes, which catalyze the same reaction but have structural dissimilarities, to function in alternative cellular compartments and metabolic pathways, we examine here the ability of Cit1p, normally found in mitochondria, to function in the cytosol, and the ability of Cit2p, normally found in peroxisomes, to function in mitochondria. It is important to mention that these mislocalizations of Cit1p and Cit2p had already been performed by Singh et al. (6) in the context of the study of topogenic signals in peroxisomal CS, but neither metabolic studies nor effects on Krebs TCA cycle function were reported. Moreover, we have purified Cit1p, Cit2p, and Mdh1p in order to test the ability of Cit1p and Cit2p to interact *in vitro* with Mdh1p in the presence of PEG as it was previously shown with pig enzymes (*20*).

EXPERIMENTAL PROCEDURES

Strains, Media and Transformation Procedures. The yeast null mutant *cit1* (*cit1::LEU2*) and *cit1cit2* (*cit1::LEU2 cit2::URA3*) strains used in this study originated from the haploid parental strain FYF5 (*MAT*α *ura3-52 leu2*Δ*1 his3*Δ*200 trp1*Δ*63*), isogenic to the reference strain S288C (ATCC 26108). The yeast media used in this study were synthetic complete (SC) media prepared as described by Sherman et al. (*21*) with either 2% glucose (SCD) or 2% sodium acetate (SCAc) as the carbon source. SCD-W was like SCD but lacking tryptophan. Rich media consisted of 1% yeast extract and 2% peptone (YP) and a carbon source: either 2% glucose (YPD), 2% (v/v) lactic acid (YPL), or 2% sodium acetate (YPAc). YPL medium contained also 1% KH_2PO_4 and was adjusted to pH 5.5 with NaOH. Two percent agar (Difco) was added for plates. Yeast transformations were conducted using the lithium acetate protocol of Gietz et al. (*22*).

The host *Escherichia coli* strain used for cloning was XL1-Blue (*recA1, end A1, gyrA96, thi-1, hsdR17, supE44, relA1, lac,* [*F′ proAB, lacIq lacZ*ΔM15, *Tn10*(*tet*^{r})]). The strain used for overproduction of histidine-tagged proteins was BL21 (*F*$^-$ *ompT gal [dcm] [lon] hsdS*$_B$ (r_B- m_B-)). Preparation and transformation of competent cells were performed according to Morrison (*23*). Bacterial transformant cells were grown on LB plates supplemented with 100 μg of ampicillin per mL.

Vectors and Primers. All the constructs were cloned in either pRS314 (ARS-CEN) or pRS424 (2μ), yeast/bacterial shuttle vectors containing the yeast *TRP1* gene as a selectable marker (*24*). Plasmids used as templates for PCR amplification of *CIT1* and *CIT2* fragments were YEp352/CS1 (*25*) and pBR322/CS2 (pBR322 bearing the *CIT2* gene), respectively. Vector pPROEX-1, a bacterial expression plasmid with a sequence encoding an N-terminal 6xHis tag and a recognition site for the TEV protease to make removal of the 6xHis tag possible (Life Technologies), was used for bacterial overproduction of the histidine-tagged Cit1p, Cit2p, and Mdh1p and their subsequent affinity purification on a nickel-agarose column.

The oligonucleotides were obtained from Gibco-BRL or IDT and are listed below from 5′ to 3′ with the restriction sites in italics:

CIT1P-5′-Kpn: GG*GGTACC*AAAAGGCGTCACGTT-TTTTTCCGC

CIT1P-3′-Xho: CCG*CTCGAG*CATCTTCGAAATA-GTATTATATTGCTAT

CIT1PLS-3′-Nhe-Pst: AA*CTGCAG*AACTA*GCTAGC*-GCTACTATAGTGGCGAGCAT

δLSCIT1-5′-Nhe: CCCTA*GCTAGC*GAACAAACGT-TGAAGGAGAGATT

δLSCIT1-5′-Xho: CCG*CTCGAG*GCCTCCGAACAA-ACGTTGAAGGA

δLSCIT1-5′-Sac: CCATGG*GAGCTC*GCCTCCGAA-CAAACGTTGAAGGAGAGATTTGC

CIT1-3′-Xho: CCG*CTCGAG*CTATTAGTTCTTACTT-TCGATTTTCTTTAC

CIT2-5′-Nhe: CCCTA*GCTAGC*ATGACAGTTCCTT-ATCTAAATTCAAAC

CIT2-5′-Sac: CCATGG*GAGCTC*ATGACAGTTCCT-TATCTAAATTCAAAC

CIT2δSKL-3′-Xho-Pst: AA*CTGCAG*AACCG*CTCG-AG*TTACTATTCAATGTTTTTGACCAATTCCTTGT

CIT2SKN-3′-Xho: CCG*CTCGAG*CTAGTTTTTGCTT-TCAATGTTTTTGACCAATTC

CIT2-3′-Xho: CCG*CTCGAG*CTATAGTTTGCTTTC-AATGTTTTTGAC

CIT1T-5′-Xho: CCG*CTCGAG*GGAAAATTTGATTT-TTGATTCAGGG

CIT1T-3′-Pst: AA*CTGCAG*GTTCATATACATATA-AACG

MDH1-5′-Ehe: GGAATTCCATATG*GGCGCC*TAT-AAAGTGACTGTTTTGGGTGCAG

MDH1-3′-Xho: CCG*CTCGAG*CTCTATTTACTAGC-AACAAAGTTGAC

Plasmid Constructions. All enzymatic reactions were performed as recommended by the manufacturers (Boehringer Mannheim, Gibco-BRL, Qiagen and Stratagene) and all recombinant manipulations were done according to Maniatis et al. (*26*). Plasmids were prepared using commercially available kits (Qiagen, Promega). Cloned Pfu polymerase (Stratagene) was used in all polymerase chain reaction (PCR) amplifications.

The 495-bp CIT1PLS fragment that includes 375-bp of the *CIT1* 5′-flanking region (promoter, P) and the sequence encoding the first 40 amino acids (leader sequence, LS) was PCR-amplified using the primers CIT1P-5′-Kpn and CIT1PLS-3′-Nhe-Pst, digested with *Kpn*I and *Pst*I and inserted between the corresponding sites of pRS314 to generate the plasmid pRS-C-CIT1PLS. Primer CIT1PLS-3′-Nhe-Pst contains 3 mismatches (in codons 39 and 40) creating an *Nhe*I site without changing the amino acid sequence. The 1383-bp fragment corresponding to the *CIT2* open reading frame (ORF) without the three codons (Ser-Lys-Leu) from the carboxyl-terminal end was PCR-amplified using the primers CIT2-5′-Nhe and CIT2δSKL-3′-Xho-Pst, digested with *Nhe*I and *Pst*I, and inserted between the corresponding sites of pRS-C-CIT1PLS to generate pRS-C-CIT1PLS-CIT2. Finally, the 332-bp fragment containing the 3′-flanking region of *CIT1* (terminator, T) was generated by PCR using the primers CIT1T-5′-Xho and CIT1T-3′-Pst, digested with *Xho*I and *Pst*I, and inserted between the corresponding sites of pRS-C-CIT1PLS-CIT2. The resulting plasmid, bearing the gene encoding Cit2p without its SKL peroxisomal targeting sequence and fused to the mitochondrial targeting sequence of Cit1p, was designated pRS-C-LSCIT2δSKL. On the basis of the Cit1p sequence, which ends in SKN and yet is directed to mitochondria, we have constructed another version of the previous plasmid where the three last codons of *CIT2* ORF encode SKN (instead of SKL), to make minimal but sufficient modifications of native Cit2p to target it to mitochondria. For this purpose, the *CIT2* coding region where the last codon CTA (Leu) was replaced with a AAC (Asn) codon was generated by PCR using the primers CIT2-5′-Nhe and CIT2SKN-3′-Xho. The PCR product was digested with *Nhe*I and *Xho*I and used to replace the 1383-bp *Nhe*I-*Xho*I fragment from pRS-C-LSCIT2δSKL. The resulting plasmid was designated pRS-C-LSCIT2SKN. As a positive control, vector pRS-C-CIT1, encoding native Cit1p, was constructed. To do so, the *CIT1* coding region without the first 40 codons (leader sequence) was generated by PCR using the primers δLSCIT1-5′-Nhe and CIT1-3′-Xho. The 1329-bp PCR product was digested with *Nhe*I and *Xho*I, then used to replace the 1383-bp *Nhe*I-*Xho*I fragment from pRS-C-LSCIT2δSKL.

The *CIT1* promoter region (P, 375-bp) was PCR amplified using the primers CIT1P-5′-Kpn and CIT1P-3′-Xho, digested with *Kpn*I and *Xho*I and inserted between the corresponding sites of pRS314 and pRS424 to generate the plasmids pRS-C-CIT1P and pRS-E-CIT1P, respectively. A 1658-bp fragment containing the *CIT1* ORF without the 40 first codons plus the 3′-flanking region of *CIT1* was PCR amplified using the primers δLSCIT1-5′-Xho and CIT1T-3′-Pst, digested with *Xho*I and *Pst*I, then cloned between the corresponding sites of pRS-C-CIT1P and pRS-E-CIT1P. The resulting plasmids were designated pRS-C-δLSCIT1 and pRS-E-δLSCIT1, respectively.

To overproduce in bacteria Cit1p, Cit2p, and Mdh1p fused to 6xHis tags at their amino termini, *CIT1* ORF without its first 40 codons, full-length *CIT2* ORF, and *MDH1* ORF without its first 17 codons, were generated by PCR using the primer pairs δLSCIT1-5′Sac and CIT1-3′-Xho, CIT2-5′-Sac and CIT2-3′-Xho, MDH1-5′-Ehe and MDH1-3′-Xho, respectively. The PCR products were digested either with *Ecl*136II (an isoschizomer of *Sac*I generating blunt ends) and *Xho*I for the *CIT1* and *CIT2* PCR products, or with *Ehe*I and *Xho*I for the *MDH1* PCR product and cloned between the *Ehe*I and *Xho*I sites of pPROEX-1. The resulting plasmids where the transcription of the genes encoding the recombinant proteins of interest is governed by an IPTG-inducible *trc* promoter, were designated pPROEX-CIT1, pPROEX-CIT2, and pPROEX-MDH1, respectively.

All the constructs were sequenced using dideoxy chain termination (*27*) on an ABI 377 automated sequencer.

Yeast Cellular Fractionation. The method used to prepare mitochondria was derived from that of Daum et al. (*28*). SCD or SCD-W media (2.5 mL) were inoculated with a single colony of the appropriate strain and grown at 30 °C for about 30 h. This preculture was used to inoculate 750 mL of YPL media (in a Fernbach flask) and the culture, monitored at OD_{600nm}, was grown at 30 °C (for approximately 20 h) up to early log phase ($OD_{600nm} = 1$). The cells were harvested by centrifugation for 5 min at 4 °C, washed in water, resuspended in 2 mL/g of cells of 100 mM Tris-H_2SO_4 (pH 9.4) and 500 mM β-mercaptoethanol, and incubated for 10 min at 30 °C. After centrifugation, the cells were washed in 20 mL of 1.35 M sorbitol, then resuspended in 6 mL/g of cells of 1.35 M sorbitol and 20 mM potassium phosphate (pH 7.4) supplemented with 1 mM phenylmethylsulfonyl fluoride (PMSF). The cell wall was digested at 30 °C (with gentle agitation) in the same buffer containing 1200 units of lyticase (Sigma) per mL of suspension, until 90% cell lysis was achieved (about 20 min). The percentage of cells lysed was followed spectrophotometrically at 600 nm by diluting 20 μL of the cell suspension in 980 μL of water prior to and after digestion. The hypotonic shock due to this dilution causes breakage of the cells whose walls were digested and a consequent decrease in the absorbance. All the subsequent steps were carried out at 4 °C. After digestion, the spheroplasts were harvested by centrifugation for 5 min at 3000*g*, washed in 20 mL of 1.35 M sorbitol, and resuspended in 10 mL of buffer H (0.6 M mannitol, 10 mM Tris-HCl pH 7.4, 1 mM PMSF). After gentle homogenization, cell debris were removed by centrifugation for 10 min at 750*g*. The resulting supernatant was centrifuged for 10

min at 11000*g* to produce the first pellet of mitochondria, the new supernatant being the soluble cytosolic fraction. The pellet resulting from the previous centrifugation of cell debris was then suspended in 20 mL of buffer H, homogenized and cleared again of cell debris by centrifugation for 10 min at 750*g*. The supernatant was centrifuged for 10 min at 11000*g* to pellet the remaining mitochondria. To remove non-mitochondrial contaminants, the two pellets of mitochondria were twice resuspended together in 3 mL of buffer H, homogenized and centrifuged for 10 min at 11000*g*. The final pellet of isolated mitochondria was suspended in 300−500 μL of 10 mM Tris-HCl, pH 7.4.

SDS-PAGE and Immunoblotting. Proteins were separated on an 8.75% gel as described by Laemmli (*29*), using a Bio-Rad minigel apparatus. Cytosolic proteins were precipitated in the presence of 10% trichloroacetic acid for 15 min on ice, pelleted by centrifugation (15000*g*, 20 min, 4 °C), washed in 200 μL of acetone, centrifuged again for 5 min, and finally suspended in 20 μL of loading buffer. After electrophoresis, the separated proteins were transferred to nitrocellulose (Protran BA, Schleicher & Schuell). The nitrocellulose blot was incubated for 30 min with 3% bovine serum albumin in PBS, and for 2 h with a rabbit anti-Cit1p polyclonal antibody diluted in PBS containing 0.05% Tween 20 (PBS-T), washed in PBS-T, incubated for 1 h with secondary antibody (anti-rabbit IgG coupled to alkaline phosphatase, Promega) diluted 5000-fold in PBS-T, and washed in 50 mM Tris-HCl (pH 7.4), 200 mM NaCl. Blots were stained by incubation in 100 μg/mL NBT and 50 μg/mL BCIP in 100 mM Tris-HCl (pH 9.5), 100 mM NaCl, 5 mM $MgCl_2$. At the dilution used, the Cit1p antiserum cross-reacts with Cit2p.

Enzyme Assays and Protein Concentrations. CS activities were determined by monitoring the reaction using DTNB at 412 nm as previously described (*30*). NAD-specific isocitrate dehydrogenase activities were measured as previously described (*31*). All reactions were measured at room temperature. Protein concentrations were determined spectrophotometrically at 562 nm using the BCA protein assay as described by Smith et al. (*32*), with bovine serum albumin as the standard.

Production and Purification of the Histidine-Tagged Cit1p, Cit2p, and Mdh1p. Ten mL of LB medium containing 100 μg/mL ampicillin was inoculated with a single colony of bacterial transformant strain and incubated overnight with agitation at 37 °C. The next morning, 7.5 mL of the overnight culture was used to inoculate 750 mL of LB medium with 100 μg/mL of ampicillin. The culture was grown with agitation at 37 °C and the growth was monitored by its OD_{600nm}. At 0.5−1.0 OD_{600nm}, the expression was induced by the addition of 0.6 mM IPTG, and the cells were grown an additional 3 h at 37 °C for Cit1p and Cit2p, and 24 h at 25 °C for Mdh1p. Cells were harvested by centrifugation at 10000*g* for 10 min. The cell pellets were washed with 50 mM NaCl, centrifuged again at 10000*g* for 10 min, and stored at −70 °C. Eight cultures, each of 750 mL, were used for each purification.

The first step of enzyme isolation on a nickel-agarose column (Qiagen) was performed from either 20 g (for Cit1p1 and Cit2p) or 40 g (for Mdh1p) of frozen cells according to the procedure previously described (*17*). The fractions containing either CS or MDH activity were pooled and precipitated by adding 70% (w/v) solid ammonium sulfate.

To further purify Cit1p, the pellet was resuspended in 100 mM potassium phosphate buffer (pH 7.5) containing 1 M ammonium sulfate, then loaded onto a 20 mL phenyl sepharose column (Pharmacia) previously equilibrated with the same solution. A flow rate of 1 mL/min was used and 5 mL fractions were collected. The column was washed with 100 mL of the same solution. The fractions containing CS activity were eluted with a 1 M to 0 M ammonium sulfate gradient, pooled, and precipitated by adding 70% solid ammonium sulfate. The pellet was suspended in 100 mM Tris-HCl buffer (pH 7.5) and desalted by using a PD10 column (Pharmacia). The fractions containing Cit1p were pooled, concentrated with a centriprep 30 (Amicon) and kept at −20 °C in 100 mM Tris-HCl pH 7.5 in the presence of 10% glycerol.

For further purification of Cit2p and Mdh1p, the pellets were resuspended in 100 mM Tris-HCl buffer (pH 7.5) and loaded onto a gel filtration Sephacryl S200 column (Pharmacia) connected to an FPLC system, previously equilibrated with the same buffer. A flow rate of 0.5 mL/min was used and 0.8 mL fractions were collected. Fractions containing either CS or MDH activity were pooled, concentrated with a centriprep 30 (Amicon), and kept at −20 °C in 100 mM Tris-HCl pH 7.5 in the presence of 10% glycerol. The Sephacryl S200 column was calibrated using thyroglobulin (670 kDa), bovine γ-globulin (158 kDa), transferrin (75 kDa), phosphorylase B (100 kDa), ovalbumin (44 kDa), myoglobin (17 kDa), and vitamin B12 (1.35 kDa).

In Vitro Protein Interaction in the Presence of PEG. Enzyme mixtures were incubated for 1 h at 10 °C in 500 mM potassium phosphate buffer (pH 7.0) containing 14% PEG (w/v). The interaction was reflected by an increase of the turbidity followed spectrophotometrically at 650 nm, as previously described by Halper and Srere (*20*).

Creation of the Three-Dimensional Structure Models of Yeast Citrate Synthases. Suitable coordinate files on which to base modeling were located using a text search of the Brookhaven Protein Data Bank to identify mammalian equivalents of the yeast enzymes. Coordinates of a monomer of the open form of the pig mitochondrial CS (PDB entry 1CTS) (*33*) were used to make Cit1p and Cit2p models. The yeast protein sequences and the file name of the Brookhaven file were submitted to the SWISS−Model www server (http://expasy.hcuge.ch/swissmod/SWISS-MODEL.html; *34*) using the "first approach" mode with no special modification. Following automated sequence alignment, model-building and energy minimization, output was received via e-mail, and included coordinate files (in PDB format) of the yeast proteins, modeled on the pig mitochondrial one, and a record of the operations performed to create them. Pig mitochondrial CS had a sequence identity of 61% with Cit1p and 59% with Cit2p. Since CS functions only as a dimer, this was constructed by overlaying the yeast C-alpha coordinates on the A monomer of the crystallographically determined pig CS dimer and transforming the yeast coordinates accordingly for all its atoms, then by repeating the process for the B monomer. Transformations and subsequent color-coding of the molecule were performed using EDPDB (*35*). Some steric clash of the constructed models with the opposite monomer occurred in the region around residues 20−40. This is not

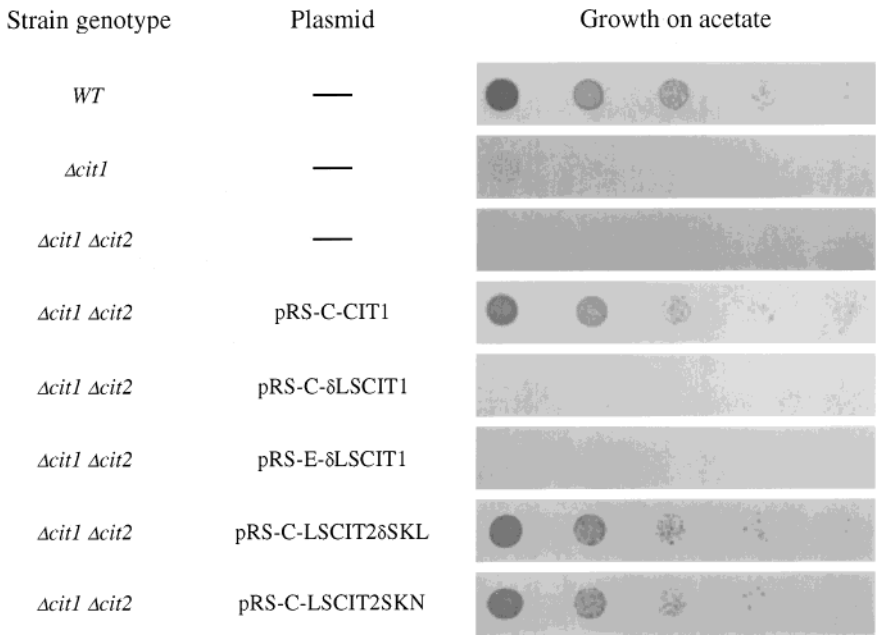

FIGURE 1: Ability of the plasmid-borne constructs to restore the growth on acetate of the double Δ*cit1* Δ*cit2* mutant. Strains were grown overnight in liquid synthetic complete glucose medium (SCD) or SCD lacking tryptophan (SCD-W, to maintain the selection pressure for the plasmids), washed twice in sterile water and resuspended to 2×10^7 cells/mL in water (1 unit OD_{600} corresponds to 2.4×10^7 cells/mL for the haploid strains used in this study). This resuspension was then serially diluted in 10-fold steps, down to 2×10^3 cells/mL. For each strain, 5 μL from each dilution (10^5 to 10 cells from the left to the right) were spotted onto synthetic complete medium with sodium acetate as a carbon source (SCAc). The plates were photographed after incubation at 30 °C for 4 days. Plasmids are described under Experimental Procedures. Genotype *WT*: Wild-type (parental strain FYF5).

unexpected, since SWISS−Model does its minimization on one monomer only, and this terminal part of CS packs primarily against the opposite monomer in an area that is distant from the active site and from the proposed MDH-binding surface. The building of molecular surfaces and the calculation of the electrostatic potentials were carried out with the program GRASP (*36*).

RESULTS

Growth on Acetate. The yeast null mutants Δ*cit1* and Δ*cit1* Δ*cit2* do not grow on acetate as the sole carbon source (*37*). These two mutants were transformed with the plasmids pRS-C-CIT1, pRS-C-δLSCIT1, pRS-C-LSCIT2δSKL, and pRS-C-LSCIT2SKN encoding native Cit1p (positive control), Cit1p without mitochondrial targeting sequence (δLSCit1p), Cit2p fused to Cit1p presequence and lacking the carboxyl-terminal tripeptide SKL (LSCit2pδSKL), and Cit2p fused to Cit1p presequence and ending in SKN (instead of SKL) (LSCit2pSKN), respectively. According to Singh et al. (*6*), deletion of the C-terminal tripeptide SKL of Cit2p is sufficient to missort this enzyme to mitochondria. However, we have combined this deletion with a fusion to the Cit1p leader sequence in order to ensure efficient mitochondrial localization of Cit2p. All these plasmids were constructed from pRS314 (*24*), a centromere-based vector carrying the yeast *TRP1* gene as a selectable marker (cf. Experimental Procedures). In all the constructs, the 5′- and 3′-flanking regions being the same (promoter and terminator of *CIT1*), the mRNAs encoding the different Citp proteins should have the same level of expression and stability, so that equivalent amounts of the plasmid-encoded Citp proteins are expected to be produced. A multicopy version of pRS-C-δLSCIT1, pRS-E-δLSCIT1, was also obtained by cloning the construct encoding δLSCit1p in pRS424, a 2-μm multicopy yeast vector with the *TRP1* gene as a marker for selection (*24*). The transformants were selected on synthetic complete glucose medium without tryptophan (SCD-W) and tested for their ability to grow on acetate (medium SCAc). The same complementation results were obtained with both mutants, and only those obtained with the double mutant are shown (Figure 1).

As expected, the construct encoding native Cit1p fully restored the ability of the mutant to utilize acetate. However, no complementation was observed with the construct encoding δLSCit1p. On the other hand, both constructs encoding LSCit2p (without the carboxyl-terminal SKL or with SKN) restored the growth of the mutant to the wild-type level. To obtain more precise information on the ability of the different transformants to grow on acetate, a growth curve in rich acetate medium (YPAc) has been performed for each as well as for wild-type and mutant (single Δ*cit1* and double Δ*cit1* Δ*cit2*) strains as positive and negative controls, respectively. As illustrated in Figure 2, no significant difference was observed between the transformant expressing native Cit1p and those expressing the mutated forms of Cit2p, and absolutely no growth was detectable with the transformant expressing δLSCit1p.

Cellular Localization and Activity of Mutant Forms of Cit1p and Cit2p. To examine cellular localization of mutant forms of Cit1p and Cit2p, mitochondrial and cytosolic fractions from yeast transformants containing chromosomal disruptions of *CIT1* and *CIT2* loci and harboring the plasmids pRS-C-δLSCIT1, pRS-C-LSCIT2δSKL, or pRS-C-LSCIT-2SKN were prepared as described under Experimental Procedures. These fractions were used for CS activity measurements (Table 1) and immunoblot analysis (Figure 3) with anti-Cit1p antiserum (which cross-reacts with Cit2p). Mitochondrial and cytosolic extracts from the transformant

Table 1: Intracellular Distribution of Citrate Synthase (CS) and NAD-Dependent Isocitrate Dehydrogenase (IDH) Activities

		CS[a]			IDH[a]		
strain genotype	plasmid	mitochondria[b]	cytosol[b]	%[c]	mitochondria[b]	cytosol[b]	%[c]
WT		1800 ± 310	48 ± 18	19 ± 1	1065	21	7
Δ*cit1*		11 ± 5	20 ± 8	94 ± 2	369	5	8.5
Δ*cit1* Δ*cit2*		26 ± 10	4 ± 3	?[d]	315	8	8
Δ*cit1* Δ*cit2*	pRS-C-CIT1	3640 ± 509	120 ± 50	23 ± 9	822	15	6.6
Δ*cit1* Δ*cit2*	pRS-C-δLSCIT1	40 ± 15	100 ± 44	93 ± 5	585	12	6
Δ*cit1* Δ*cit2*	pRS-E-δLSCIT1	94 ± 34	424 ± 107	97 ± 1	423	6	6.2
Δ*cit1* Δ*cit2*	pRS-C-LSCIT2δSKL	469 ± 82	8 ± 5	7 ± 3	685	8	3
Δ*cit1* Δ*cit2*	pRS-C-LSCIT2SKN	1010 ± 145	75 ± 23	34 ± 8	730	13	5.6

[a] Specific activities are expressed in nmoles of citrate (for CS) or NADH (for IDH) formed per min per mg of mitochondrial or cytosolic proteins± standard error of two or three independent experiments. [b] Mitochondrial and cytosolic extracts were prepared from cells grown in rich lactate medium (YPL) and harvested in early log phase (OD600 ≈ 1), as described under Experimental Procedures. [c] % represents the percentage of total cytosolic activity in relation to total cellular activity (mitochondrial + cytosolic). [d] Because of the high relative uncertainty on cytosolic specific activity in this strain, it was not possible to estimate the percentage of total cytosolic activity.

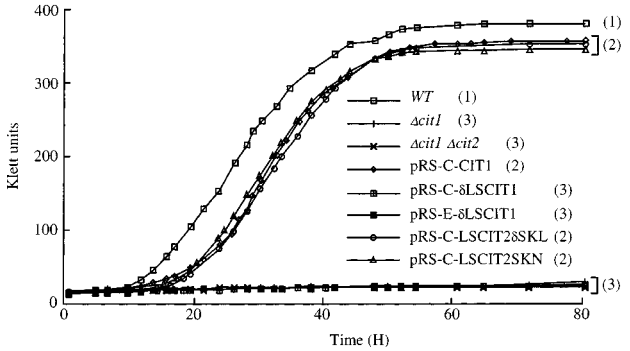

FIGURE 2: Growth curves in rich acetate (YPAc) medium. The Δ*cit1* Δ*cit2* transformants harboring the indicated plasmid as well as the parental wild type (*WT*) and mutant (single Δ*cit1* and double Δ*cit1* Δ*cit2*) strains have been grown in rich medium containing 2% acetate as the sole carbon source (YPAc). Culture growth rates were monitored by turbidity measurements using a Klett Photometer (Monostat Corp., New York, NY) with a KS-59 filter. Cells from overnight 2.5 mL SCD or SCD-W precultures were harvested by centrifugation, washed twice in sterile water, and used to grow up the final YPAc cultures with an initial OD_{600} of 0.03 (corresponding to 5 to 10 Klett units). Numbers in parentheses refer to the different groups of overlapping growth curves.

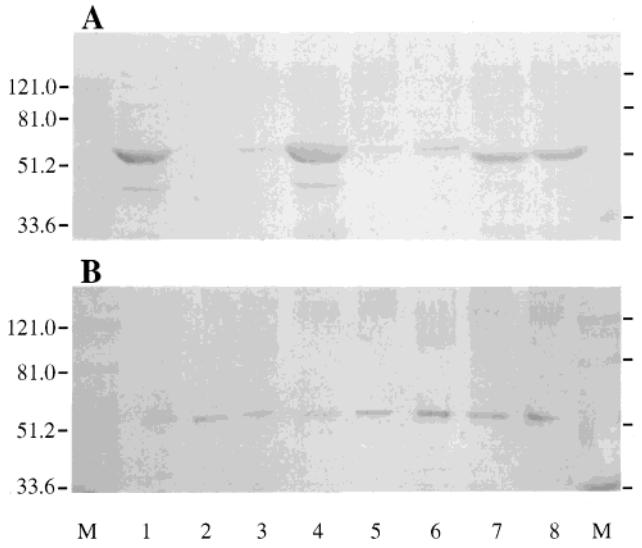

FIGURE 3: Cellular localization of mutant forms of Cit1p and Cit2p. Protein extracts corresponding to equivalent amounts of cellular material (7 units OD_{600}) from mitochondrial (A) and cytosolic (B) fractions prepared from wild-type strain (lane 1), single Δ*cit1* mutant (lane 2), and double Δ*cit1* Δ*cit2* mutant before (lane 3) and following transformation with pRS-C-CIT1 (lane 4), pRS-C-δLSCIT1 (lane 5), pRS-E-δLSCIT1 (lane 6), pRS-C-LSCIT2δSKL (lane 7), or pRS-C-LSCIT2SKN (lane 8), grown in rich lactate (YPL) medium to early log phase, were subjected to immunoblot analysis with anti-Cit1p antiserum as described under Experimental Procedures. Numbers on the left indicate the size (in kDa) of the SDS-PAGE standards of lanes M (Bio-Rad, broad range). Please note that the same amount of cellular material, and not the same amount of protein, has been loaded on each lane in order to obtain a pattern representative of the real distribution *in vivo*. Since the specific CS activities are expressed per mg of protein, the comparison of the patterns for two different strains can be correlated to the comparison of their cellular CS activity distributions only if the amount of cellular material loaded on the gel corresponds, for these two strains, to equivalent amounts of protein.

harboring the plasmid pRS-C-CIT1 (encoding native Cit1p) as well as from wild-type and original mutant strains (without any plasmid) were also analyzed as controls.

To estimate the efficiency of the fractionation, the activities of NAD-dependent isocitrate dehydrogenase (IDH), a mitochondrial marker enzyme, were determined in the mitochondrial and cytosolic fractions. As shown in Table 1, more than 90% of IDH activity was found in the mitochondria. The remainder of this activity, found in the cytosol, is indicative of a slight variable mitochondrial contamination of the cytosolic fractions. The distribution of CS activity in the single Δ*cit1* mutant where 94% of total activity fractionated with the cytosol (Table 1), was as previously reported by Rosenkrantz et al. (*3*). However, for the wild-type strain, about 80% of total activity was found to be associated with mitochondria, whereas the previous authors reported a value of only 62%. This divergence is likely due to the utilization by these authors of a different yeast strain and different growth conditions (synthetic glucose instead of rich lactate). For the transformant expressing the plasmid-encoded native Cit1p, immunochemical levels in mitochondrial extracts (Figure 3A, lane 4) are higher than those in extracts from the parental wild-type strain (Figure 3A, lane 1). The amounts of mitochondrial protein loaded on the gel for these two strains being equivalent (60 μg), this pattern is consistent with the levels of specific CS activity found in the mitochondrial extracts of these two strains (Table 1) and is likely due to the fact that a centromere-based plasmid is generally present in slightly more than one copy per cell. The double mutant has a low but significant mitochondrial CS activity (Table 1) that may be due to Cit3p (cf. Introduction).

The two mutant forms of Cit2p (LSCit2pδSKL or LSCit2pSKN) showed the same distribution pattern (Figure 3, lanes 7 and 8) with a predominantly mitochondrial

localization. The amounts of protein loaded on the gel from the transformants expressing these two mutant forms of Cit2p being equivalent (85 and 520 μg for mitochondrial and cytosolic fractions, respectively), and the immunochemical levels in the mitochondrial extracts as well as in the cytosolic extracts of these two transformants being similar, an analogous pattern of specific CS activity distribution for these two strains was expected, with similar activities between their mitochondrial and between their cytosolic fractions. As shown in Table 1, the greater part of CS activity was indeed associated with mitochondria in both cases, but the specific activites obtained with the protein ending in SKN (encoded by pRS-C-LSCIT2SKN) were about two and 10 times more than the ones obtained with the protein lacking SKL (encoded by pRS-C-LSCIT2δSKL) in mitochondrial and cytosolic fractions, respectively. Moreover, we noticed that the latter protein was very unstable and lost up to 80% of its activity in 24 h, whereas the one encoded by pRS-C-LSCIT2SKN was perfectly stable and retained 100% of its activity after several days. To determine if this difference could be attributed to the tripeptide SKN (the only difference between these two proteins), we constructed a mutated form of Cit1p where the carboxyl-terminal SKN was deleted. Surprisingly, this protein behaved exactly as native Cit1p: absolutely no difference was observed with regard to intracellular localization nor to specific activity (data not shown). Aside from these unexplained data, the results shown here demonstrated that the peroxisomal CS, when mislocalized in mitochondria, is perfectly able to metabolically replace its mitochondrial isoform.

Despite low immunochemical levels in the extracts from the transformant expressing δLSCit1p lacking mitochondrial presequence (encoded by the plasmid pRS-C-δLSCIT1), this protein appeared clearly to be predominantly localized in the cytosol (Figure 3, lane 5). This was confirmed by the CS activity distribution of which 93% was found to be associated with the cytosolic fraction (Table 1). These data also indicate that mitochondrial import of Cit1p is largely but not completely ablated with removal of the presequence. Nevertheless, although Cit1p has been mainly mislocalized to the cytosol, the CS specific activity in this compartment does not permit a conclusion as to the ability of the "cytosolic" form of Cit1p to complement its absence in mitochondria. Indeed, this specific activity represents only 5% of wild-type activity whereas a collection of mutant forms of Cit1p available in the lab indicate that a minimum of 20% of wild-type mitochondrial CS activity level is required to obtain full growth on acetate. For instance, the results reported here show that the transformant expressing Cit2p lacking SKL grows fully on acetate (Figures 1 and 2) with only 26% of wild-type CS activity (Table 1). Therefore, the data obtained with the mislocalized form of Cit1p suggested that this enzyme is unstable in the cytosol compartment and that its overexpression is required for tests of metabolic function.

Multicopy Expression of "Cytosolic" Cit1p. To increase levels of expression of the "cytosolic" form of Cit1p, the multicopy plasmid encoding δLSCit1p, pRS-E-δLSCIT1, was transformed into the yeast strain lacking mitochondrial (Cit1p) and peroxisomal (Cit2p) CS (double Δ*cit1* Δ*cit2* disruption mutant). As illustrated in Figures 1 and 2, multicopy expression of this mutant form of Cit1p did not change the inability of the transformant to utilize acetate: absolutely no growth was detectable neither on synthetic acetate (ScAc) medium (Figure 1) nor in liquid rich acetate (YPAc) culture (Figure 2). However, as shown in Figure 3B, this multicopy expression significantly increased the cytosolic level of Cit1p (compare lanes 6 and 5). This was confirmed by CS activity measurements (Table 1) which showed an increase by a factor of 4 in the cytosolic specific activity in the multicopy transformant (plasmid pRS-E-δLSCIT1) when compared to the centromere-based plasmid transformant (plasmid pRS-C-δLSCIT1). This increased the cytosolic CS specific activity to more than 20% of the wild-type mitochondrial level, allowing us to conclude that the cytosolic form of Cit1p is unable to metabolically compensate its absence in mitochondria.

Ability of Cit1p and Cit2p to Interact with Mdh1p in Vitro. The results described above indicate that Cit2p, when localized in mitochondria, is able to metabolically mimic Cit1p. According to the TCA multienzyme complex idea, these data suggest that Cit2p, as well as Cit1p, would be able to contribute to this complex. Pig CS and mitochondrial MDH interact *in vitro* in the presence of PEG (*20*). More recently, experiments performed with yeast or pig enzymes indicate that CS may physically associate with MDH to ensure direct transfer of oxaloacetate (*15*−*17*). To test the ability of yeast CS enzymes, Cit1p and Cit2p, to interact with yeast mitochondrial MDH (Mdh1p) in the presence of PEG, the coding regions of the *CIT1*, *CIT2*, and *MDH1* genes have been cloned in the bacterial expression vector pPROEX-1 (where they were fused in frame, at their 5′ end, to a sequence encoding six consecutive His residues), and the three histidine-tagged proteins were overproduced in bacteria and purified on a nickel-agarose column as described under Experimental Procedures. The specific activities of the pure enzymes were, in units per mg, 70, 104, and 900 for Cit1p, Cit2p, and Mdh1p, respectively. As illustrated in Figure 4, Cit2p as well as Cit1p interacted with Mdh1p in the presence of 14% PEG, suggesting that the peroxisomal CS isoform may be able, when mislocalized in mitochondria, to take part in the TCA multienzyme complex.

Structural Modeling and Electrostatic Properties of Cit1p and Cit2p. The ability of two isoenzymes to replace each other within a quinary structure requires that these two proteins share high structural similarities of their outer surfaces. Since high-definition structures of the yeast enzymes are not available, models of the three-dimensional structures of Cit1p and Cit2p were generated on the basis of the known X-ray structure of pig CS, as described under Experimental Procedures. Figure 5 shows the molecular surfaces of these yeast models in three different orientations. From these pictures, it clearly appears that the two isoenzymes have a very high outer surface structural similarity so that they are almost indistinguishable from each other. Recent data indicate that another important property of the outer surfaces of CS and MDH enzymes involved in their interaction is the electrostatic potential of these surfaces. Results obtained about the channeling of oxaloacetate between pig CS and mitochondrial MDH maintained in a close proximity either in a PEG coprecipitate (*16*) or within a fusion enzyme (*17*) established the electrostatic nature of this channeling. This was an experimental confirmation of previous Brownian dynamics simulations performed on a

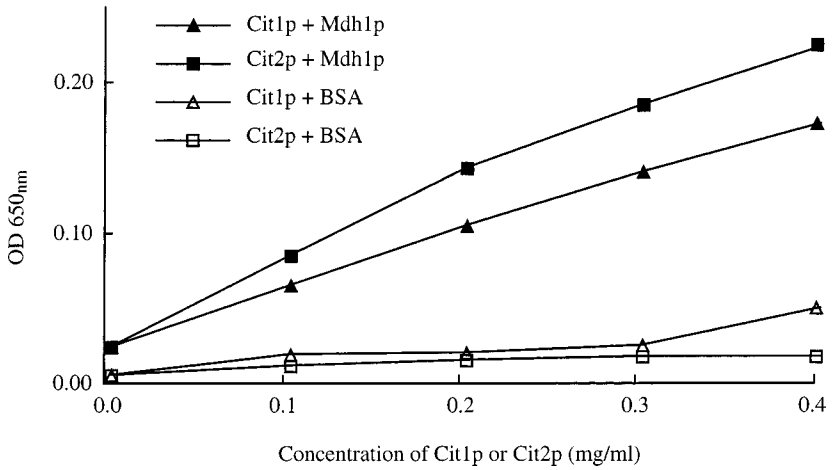

FIGURE 4: Ability of Cit2p to interact with Mdh1p in the presence of PEG. Protein mixtures containing 0.2 mg/mL of either Mdh1p or BSA (as a negative control) were incubated in the presence of increasing amounts of Cit1p or Cit2p for 1 h at 10 °C, in 500 mM potassium phosphate buffer (pH 7.0) containing 14% PEG (w/v). The turbidity was followed spectrophotometrically at 650 nm.

model of the pig fusion enzyme, which showed that a positive electrostatic surface potential between the active sites of the fusion protein, could account for the channeling of oxaloacetate (*18*). Moreover, a model of a docking orientation between pig CS, mitochondrial MDH, and mitochondrial aconitase showed substantial interacting surface areas with spatial and electrostatic complementarities, which made the complex thermodynamically favorable (*38*). The electrostatic potentials of the model structure surfaces of Cit1p and Cit2p have been calculated. As shown in Figure 5, there is an overwhelming similarity between the electrostatic profiles of the two isozyme surfaces. Especially, no significant difference could be noticed between the two upper pictures representing the surfaces of Cit1p and Cit2p that are proposed to interact with Mdh1p based on the model published for the pig enzymes (*18*, *38*). Although the structural similarity between the two models is primarily a result of both sequences being fit to the same template structure, the observed electrostatic similarity has no such constraint.

DISCUSSION

Results obtained in this study indicated that, in the yeast *Saccharomyces cerevisiae*: (a) a mislocalized cytosolic form of normally mitochondrial CS, Cit1p, is unable to bypass the block in the TCA cycle that results from its absence in mitochondria; (b) the peroxisomal CS, Cit2p, when mislocalized in mitochondria, is able to replace its mitochondrial isoform Cit1p for a fully functional Krebs TCA cycle; (c) Cit2p has the same ability as Cit1p to interact *in vitro* with the mitochondrial MDH, Mdh1p, in the presence of 14% PEG.

Expression of native Cit1p in the mitochondria of a mutant containing chromosomal disruptions of *CIT1* and *CIT2* loci (encoding Cit1p and Cit2p, respectively) using a centromere-based plasmid gave rise to higher cellular levels of this enzyme than those observed in a wild-type strain. However, to express the mislocalized cytosolic form of Cit1p, use of a multicopy expression vector was found to be necessary to obtain significant cytosolic levels (namely, a little bit more than 20% of the mitochondrial wild-type level, which is the minimum of mitochondrial CS activity required to allow the corresponding strain to grow fully on acetate). This is presumably due to instability and rapid turnover of the protein Cit1p in that compartment. Interestingly, the same phenomenon was observed previously with the cytosolic expression of a mislocalized form of normally mitochondrial Mdh1p (*39*), whereas a mislocalized form of normally peroxisomal Mdh3p was found to be stably expressed in the cytosol (*40*). As mentioned by Small and McAlister-Henn (*39*), a possible explanation for this discrepancy is that peroxisomal proteins are normally folded in the cytosol prior to organellar import, whereas the majority of mitochondrial proteins are folded following import (*41*−*43*). Thus, there may be differences in the rates of correct folding of cytosolic forms of normally mitochondrial and peroxisomal proteins which could account for the observed stabilities.

The cytosolic form of Cit1p was found to be incompetent to restore growth of a Δ*cit1* (or Δ*cit1* Δ*cit2*) strain on acetate medium. A priori, this may appear as an expected result since it is already known that Cit2p does not support TCA cycle activity. However, this absence of cross-complemetation may be due to the peroxisomal localization of Cit2p. On the other hand, all the factors that would be required to allow a cytosolic CS activity to bypass its absence in mitochondria are present in yeast: the citrate transporter allows citrate, the main product of the CS reaction, to cross the inner mitochondrial membrane, and the combination of the inner mitochondrial membrane malate transporter and cytosolic MDH (Mdh2p) similarly can supply oxaloacetate, the CS substrate, to the cytoplasm. That this bypass does not in fact occur suggests that the presence of the CS enzyme itself is required in the mitochondria to get a functional Krebs TCA cycle. This is consistent with the results obtained by Kispal et al. (*12*), showing that growth of Δ*cit1* mutant cells on acetate can be restored by transformation of these cells with a plasmid encoding a catalytically inactive Cit1p. It has been shown that Cit1p interacts with the mitochondrial citrate transporter (*44*). This interaction has even been used to purify the transporter from *S. cerevisiae* with an affinity column containing pig heart CS (*45*). Moreover, Sandor et al. (*46*) have shown that normal citrate uptake by mitochondria requires specific cooperation between Cit1p and the citrate transporter. These data may explain the results obtained by Kispal et al. (*12*) and those reported here. In fact, all of the enzymes of the TCA cycle are bound to the inner surface of

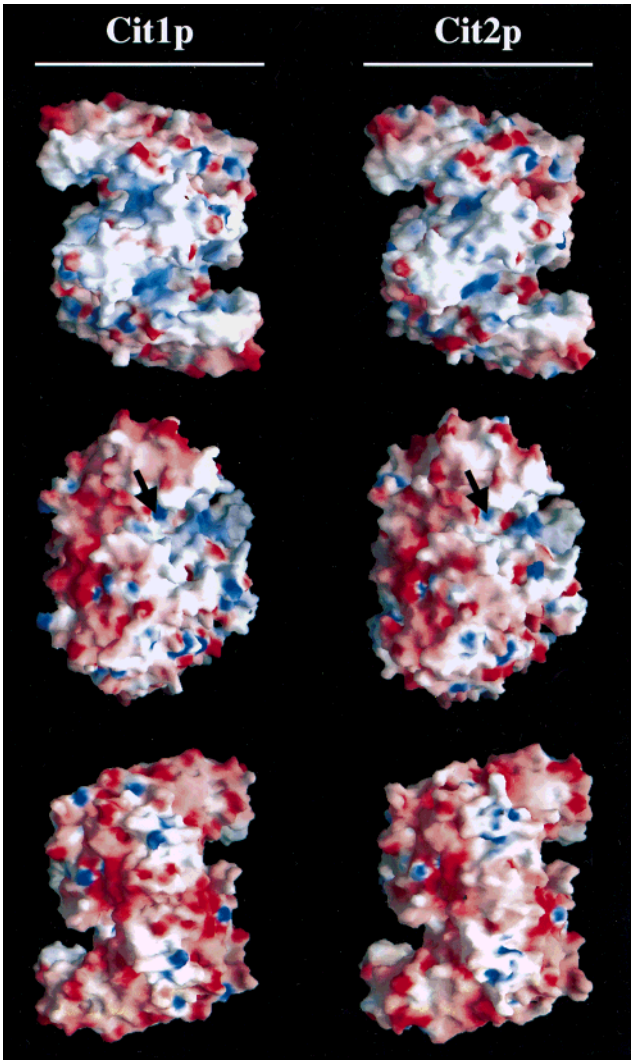

FIGURE 5: Molecular surfaces and electrostatic potentials of Cit1p and Cit2p models. The three-dimensional structures of the yeast proteins Cit1p and Cit2p were modeled using the X-ray coordinates of the pig heart CS as the initial template, as described under Experimental Procedures. The molecular surfaces are colored according to the electrostatic potential calculated at zero ionic strength. Blue areas represent electrostatically positive regions; red, electrostatically negative regions (limits set at ± 15 kT). Titratable residues were assumed to be in their usual protonation state at pH 7, i.e., the net charge of all Asp and Glu residues was set to −1e and all Arg and Lys residues set to +1e. All histidines were in their neutral form. For each protein, the three pictures represent three different orientations obtained by successive 90° rotations about a horizontal axis. The arrows on the central pictures indicate the active site of one monomer. This figure was prepared using GRASP (*36*).

the inner mitochondria membrane (*47*−*49*) via binding proteins such as complex I for MDH, isocitrate dehydeogenase, and α-ketoglutarate dehydrogenase (*50*). These interactions are not disconnected from the idea of a TCA multienzyme complex, since they may allow the TCA enzymes to stay in a close proximity, and the inner mitochondrial membrane to play the role of a structural support for the complex.

Nevertheless, a mislocalized cytosolic form of Mdh1p was previously found to be quite competent for restoration of growth of a Δ*mdh1* mutant on acetate medium (*39*), suggesting that function in the TCA cycle does not require mitochondrial localization in this case. However, unlike citrate, oxaloacetate, the product of the MDH reaction, cannot itself cross the mitochondrial membrane. Thus, cytoplasmic oxaloacetate must be transferred to mitochondria by indirect substrate shuttles and transamination reactions. These reactions necessarily involve mitochondrial enzymes that may have the same abilities as Mdh1p to interact with Cit1p, thus allowing the import of oxaloacetate into mitochondria and a reconstitution of the complex. Interestingly, a MDH isoform, Mdh2p, is naturally present in the cytosol of *S. cerevisiae* (where it is involved in gluconeogenesis) but is unable to act as a shunt for the missing Mdh1p enzyme since a Δ*mdh1* mutant does not grow on acetate. Consistently, the ability of the mislocalized cytosolic Mdh1p to restore a wild-type phenotype in a Δ*mdh2* mutant was limited (*39*), suggesting that oxalacetate generated by Mdh2p is microcompartmentalized, i.e., forms a separate pool from that of the bulk phase in cytoplasm. Altogether, these data indicate that features other than catalytic activity may be important for gluconeogenic as well as for TCA cycle functions.

Another important result of the study reported here is the ability of the peroxisomal CS, Cit2p, when mislocalized into mitochondria, to yield a functional Krebs TCA cycle. According to the TCA multienzyme complex idea, this result was unexpected since two isoenzymes, which catalyze the same reaction, may have structural dissimilarities and may functionally differ from each other in their binding abilities. For instance, Halper and Srere (*20*) have shown that pig mitochondrial MDH, but not cytosolic MDH, binds to pig CS *in vitro* in the presence of PEG. In the same way, the oxaloacetate channeling phenomenon observed between pig CS and mitochondrial MDH coprecipitated in PEG or covalently linked within a fusion enzyme does not exist anymore when mitochondrial MDH is replaced by its cytosolic isoform (*16*, *17*). These two pig MDH isoforms have a very high structural similarity but show a strong divergence in their electrostatic surface potentials (*38*). The difference in their binding behavior is likely due to this divergence since the oxaloacetate channeling phenomenon is ionic strength-dependent, which is indicative of an electrostatically based mechanism (*16*, *17*). The idea of a functional difference between two isoenzymes also is supported by the existence of isoforms that obviously cannot replace each other, even though they normally are localized in the same organelle. This is the case in *S. cerevisiae* for CS and aconitase for which two isoenzymes encoded by *CIT1* and *CIT3* (*7*), and by *ACO1* (*51*) and *ACO2* (*52*), respectively, are present in mitochondria. Despite this redundancy, a Δ*cit1* mutant does not grow on acetate, and a Δ*aco1* mutant is petite and a glutamate autotroph (*51*). Therefore, the ability of Cit2p to metabolically replace Cit1p in mitochondria is likely due to the fact that surfaces of both isoenzymes share extremely high structural and electrostatic similarities, as illustrated in Figure 5. Concerning these modeling studies, it is important to mention that errors in the structural modeling would tend to make the surfaces look different, as would random divergence of the two proteins' sequences, particularly since solvent-exposed residues have been shown to be largely nonessential for folding and stability of individual proteins (*53*). Since Cit1p and Cit2p differ from each other in 25% of their amino acids, differences may have been expected in a few important charged residues. Consequently, the observed similarity in

their modeled electrostatic surfaces is particularly noteworthy. The similarity is supported by the ability of Cit2p to mimic Cit1p in its *in vitro* interaction in the presence of PEG.

However, it is known that Cit2p, contrary to Cit1p, does not bind to inner mitochondrial membranes (*54*). Because of the high structural resemblance between these two proteins, we repeated these binding experiments and confirmed this difference between the two isoenzymes (data not shown). Therefore, the results obtained here imply that the binding of CS to the membrane is not essential for the Krebs TCA cycle to be functional. This seems inconsistent with the observation that citrate transporter needs to interact with mitochondrial CS for full activity, as mentioned above. Nevertheless, it is possible that the interaction between the sequential TCA cycle enzymes precedes their binding to the inner membrane, and that the binding of Cit2p to the membrane is made possible *in vivo* via its interaction with Mdh1p (or aconitase).

Altogether, the results reported in this study reinforce the concept that an enzyme is much more than an active site, and a metabolic pathway is more than an assembly of enzymatic activities and metabolites.

ACKNOWLEDGMENT

We thank Virginia Poffenberger for technical assistance and Elizabeth Yetman for assistance in sequencing the constructs. We also thank Dr. Sarah A. McIntire for her critical review of this paper. C.V., S.L., I.M., and K.C.U. wish to dedicate this paper in memory of Paul A. Srere.

REFERENCES

1. Suissa, M., Suda, K., and Schatz, G. (1984) *EMBO J. 3*, 1773−1781.
2. Kim, K.-S., Rosenkrantz, M. S., and Guarente, L. (1986) *Mol. Cell. Biol. 6*, 1936−1942.
3. Rosenkrantz, M. S., Alam, T., Kim, K., Clark, B. J., Srere, P. A., and Guarente, L. P. (1986) *Mol. Cell. Biol. 6*, 4509−4515.
4. Lewin, A. S., Hines, V., and Small, G. M. (1990) *Mol. Cell. Biol. 10*, 1399−1405.
5. McCammon, M. T., Veenhuis, M., Trapp, S. B., and Goodman, J. M. (1990) *J. Bacteriol. 172*, 5816−5827.
6. Singh, K. K., Small, G. M., and Lewin, A. S. (1992) *Mol. Cell. Biol. 12*, 5593−5599.
7. Jia, Y.-K., Bécam, A.-M., and Herbert, C. J. (1997) *Mol. Microbiol. 24*, 53−59.
8. Chappell, B., and Haaroff, K. N. (1967) in *Biochemistry of mitochondria* (Slater, E. C., Kaniuga, Z., and Wojtczak, L, Eds.) pp 75−91, Academic Press, London and PWN−Polish Scientific Publishers, Warsaw.
9. Liao, X., Small, W. C., Srere, P. A., and Butow, R. A. (1991) *Mol. Cell. Biol. 11*, 38−46.
10. Liao, X., and Butow, R. A. (1993) *Cell 72*, 61−71.
11. McAlister-Henn, L., and Thompson, L. M. (1987) *J. Bacteriol. 169*, 5157−5166.
12. Kispal, G., Evans, C. T., Malloy, C., and Srere, P. A. (1989) *J. Biol. Chem. 264*, 11204−11210.
13. Srere, P. A. (1987) *Annu. Rev. Biochem. 56*, 89−124.
14. Srere, P. A. (1993)*Biol. Chem. 374*, 833−842.
15. Lindbladh, C., Rault, M., Hagglund, C., Small, W. C., Mosbach, K., Bülow, L., Evans, C., and Srere, P. A. (1994) *Biochemistry 33*, 11692−11698.
16. Morgunov, I., and Srere, P. A. (1998) *J. Biol. Chem. 273*, 29540−29544.
17. Shatalin, K., Lebreton, S., Rault-Leonardon, M., Vélot, C., and Srere, P. A. (1999) *Biochemistry 38*, 881−889.
18. Elcock, A. H., and McCammon, J. A. (1996) *Biochemistry 35*, 12652−12658.
19. Haggie, P. M., and Brindle, K. M. (1999) *J. Biol. Chem. 274*, 3941−3945.
20. Halper, L. A., and Srere, P. A. (1977) *Arch. Biochem. Biophys. 184*, 529−534.
21. Sherman, F., Fink, G. R., and Hicks, J. B. (1986) *Methods in yeast genetics*, Cold Spring Harbor Laboratory Press, Cold Spring Harbor, N. Y.
22. Gietz, D., St-Jean, A., Woods, R. A., and Schiestl, R. H. (1992) *Nucl. Acid. Res. 20*, 1425.
23. Morrison, A. (1977) *J. Bacteriol. 132*, 349.
24. Sikorski, R. S., and Hieter, P. (1989) *Genetics 122*, 19−27.
25. Lindbladh, C., Brodeur, R. D., Lilius, G., Bülow, L., Mosbach, K., and Srere, P. A. (1994) *Biochemistry 33*, 11684−11691.
26. Maniatis, T., Fritsch, E. F., and Sambrook, J. (1982) *Molecular cloning: a laboratory manual*, Cold Spring Harbor Laboratory Press, Cold Spring Harbor, N. Y.
27. Sanger, F., Nicklen, S., and Coulson, A. R. (1977) *Proc. Natl. Acad. Sci. U.S.A. 74*, 5463−5467.
28. Daum, G., Böhni, P., and Schatz, G. (1981) *J. Biol. Chem. 257*, 13028−13033.
29. Laemmli, U. K. (1970) *Nature 227*, 680−685.
30. Srere, P. A., Brazil, H., and Gonen, L. (1963) *Acta Chem. Scand. 17*, S129−S134.
31. Keys, D. A., and McAlister-Henn, L. (1990) *J. Bacteriol. 172*, 4280−4287.
32. Smith, P. K., Krohn, R. I., Hermanson, G. T., Mallia, A. K., Gartner, F. H., Provenzano, M. D., Fujimoto, E. K., Goeke, N. M., Olson, B. J., and Flenk, D. C. (1985) *Anal. Biochem. 150*, 76−85.
33. Remington, S. J., Wiegand, G., and Huber, R. (1982) *J. Mol. Biol. 158*, 111−152.
34. Peitsch, M. C. (1996) *Biochem. Soc. Trans. 24*, 274−279.
35. Zhang, X.-J., and Matthews, B. W. (1995) *J. Appl. Cryst. 28*, 624−630.
36. Nicholls, A., Sharp, K. A., and Honig, B. (1991) *Proteins 11*, 281−296.
37. Kispal, G., Rozenkrantz, M., Guarente, L., and Srere, P. A. (1988) *J. Biol. Chem. 263*, 11145−11149.
38. Vélot, C., Mixon, M. B., Teige, M., and Srere, P. A. (1997) *Biochemistry 36*, 14271−14276.
39. Small, W. C., and McAlister-Henn, L. (1997) *Arch. Biochem. Biophys. 344*, 53−60.
40. McAlister-Henn, L., Steffan, J. S., Minard, K. I., and Anderson, S. L. (1995) *J. Biol. Chem. 270*, 21220−21225.
41. Purdue, P. E., and Lazarow, P. B. (1994) *J. Biol. Chem. 269*, 30065−30068.
42. Glover, J. R., Andrews, D. W., and Rachubinski, R. A. (1994) *Proc. Natl. Acad. Sci. U.S.A. 91*, 10541−10545.
43. McNew, J. A., and Goodman, J. M. (1994) *J. Cell. Biol. 127*, 1245−1257.
44. Grigorenko, E. V., Small, W. C., Persson, L.-O., and Srere, P. A. (1990) *J. Mol. Recognit. 3*, 215−219.
45. Persson, L.-O., and Srere, P. A. (1992) *Biochem. Biophys. Res. Commun. 6*, 70−76.
46. Sandor, A., Johnson, J. H., and Srere, P. A. (1994) *J. Biol. Chem. 269*, 29609−29612.
47. D'Souza, S. F., and Srere, P. A. (1983) *J. Biol. Chem. 258*, 4706−4709.
48. Robinson, J. B., Jr., and Srere, P. A. (1985) *J. Biol. Chem. 262*, 10800−10805.
49. Brent, L. G., and Srere, P. A. (1987) *J. Biol. Chem. 262*, 319−325.
50. Sumegi, B., and Srere, P. A. (1984) *J. Biol. Chem. 259*, 8748−8752.
51. Gangloff, S. P., Marguet, D., and Lauquin, G. J.-M. (1990) *Mol. Cell. Biol. 10*, 3551−3561.
52. Vélot, C., Haviernik, P., Boucherie, H., and Lauquin, G. J.-M. (1996) in *Program and Abstracts of the Yeast Genetics and Molecular Biology Meeting*, pp 291, Madison, WI.
53. Matthews, B. W. (1995) *Adv. Protein Chem. 46*, 249−278.
54. Kispal, G., and Srere, P. A. (1991) *Arch. Biochem. Biophys. 286*, 132−137.

BI991695N